INFECTION AND IMMUNITY, Dec. 2010, p. 5043–5053 Vol. 78, No. 12
0019-9567/10/$12.00 doi:10.1128/IAI.00604-10

Constitutive MEK1 Activation Rescues Anthrax Lethal Toxin-Induced Vascular Effects *In Vivo*▽

Robert E. Bolcome III[1,2] and Joanne Chan[1,2]*

Biological and Biomedical Sciences Program[1] and Vascular Biology Program, Children's Hospital and the Department of Surgery,[2] Harvard Medical School, Boston, Massachusetts 02115

Received 4 June 2010/Returned for modification 3 July 2010/Accepted 9 September 2010

Anthrax lethal toxin (LT) increases vascular leakage in a number of mammalian models and in human anthrax disease. Using a zebrafish model, we determined that vascular delivery of LT increased permeability, which was phenocopied by treatment with a selective chemical inhibitor of MEK1 and MEK2 (also known as mitogen-activated protein kinase [MAPK] kinase, MEK, or MKK). Here we investigate further the role of MEK1/phospho-ERK (pERK) in the action of LT. Overexpression of wild-type zebrafish MEK1 at high levels did not induce detrimental effects. However, a constitutively activated version, MEK1^{S219D,S223D} (MEK1DD), induced early defects in embryonic development that correlated with increased ERK/MAPK phosphorylation. To bypass these early developmental defects and to provide a genetic tool for examining the action of lethal factor (LF), we generated inducible transgenic zebrafish lines expressing either wild-type or activated MEK1 under the control of a heat shock promoter. Remarkably, induction of MEK1DD transgene expression prior to LT delivery prevented vascular damage, while the wild-type MEK1 line did not. In the presence of both LT and MEK1DD transgene expression, cardiovascular development and function proceeded normally in most embryos. The resistance to microsphere leakage in transgenic animals demonstrated a protective role against LT-induced vascular permeability. A consistent increase in ERK phosphorylation among LT-resistant MEK1DD transgenic animals provided additional confirmation of transgene activation. These findings provide a novel genetic approach to examine mechanism of action of LT *in vivo* through one of its known targets. This approach may be generally applied to investigate additional pathogen-host interactions and to provide mechanistic insights into host signaling pathways affected by pathogen entry.

Studies on anthrax pathogenesis have defined three toxin proteins secreted by *Bacillus anthracis* that can induce severe vascular and organ damage prior to lethality in experimental models (21, 52). Anthrax toxin proteins consist of an internalization subunit, protective antigen (PA), that can couple with either of two catalytic subunits: edema factor (EF) and lethal factor (LF) (11). PA has the ability to bind host receptors with high affinity and is responsible for the internalization of EF and/or LF into the cytoplasm. Biochemical studies have revealed that EF and LF have distinct enzymatic activities. EF increases cellular cyclic AMP (cAMP) levels, and LF is a metalloprotease that can cleave and inactivate MEKs (also known as mitogen-activated protein kinase [MAPK] kinase, MEK, or MKK) (52). EF and PA constitute edema toxin (ET), while LF and PA function as lethal toxin (LT). Over the years, studies on LT have generated potent and consistent phenotypes in rodent models, including vascular leakage, lung edema, pleural effusions, and hemorrhage, before lethality (15, 21, 35, 42). Thus, we became interested in further investigating the vascular actions of LT. To do this, we developed a zebrafish embryonic model that facilitated the direct observation of LT effects on the vasculature *in vivo* (9, 28).

We previously showed that delivery of LT into the embryonic vasculature generated a distinct progression of phenotypic defects, beginning with an increase in vascular leakage (9). We further demonstrated that increased permeability was not due to endothelial cell death (9). *In vitro* and biochemical assays have shown that LF can cleave and inactivate a number of related kinases in the MEK/MKK subfamily: MEK1 to MEK4, MEK6, and MEK7 (18, 39, 47). However, the contribution of each kinase to the effects of LT has not been explored *in vivo*. We took initial steps to examine the role of this toxin's enzymatic activity in generating vascular effects in a zebrafish model. In our previous study a catalytically inactive version, LF Y728F (46), produced no phenotype, while replacement of the catalytic domain of LF with diphtheria toxin A chain (LF_NDTA) caused global cell death. In contrast, treatment of zebrafish embryos with a highly selective chemical inhibitor of MEK1 and MEK2 faithfully phenocopied the effects of LT (9), suggesting that inactivation of these MEK proteins could be a major contributor to LF-induced vascular permeability.

Previous mammalian studies have suggested that MEK1 and MEK2 may be functionally redundant (41); however, null mutations in MEK1 are recessively lethal in mice due to vascular abnormalities at embryonic day 10.5 (E10.5), while MEK2-null mice are viable, with no apparent phenotype (6, 20). Thus, we focused on a possible connection between LF and MEK1 inactivation as an important step in LT-induced vascular permeability. To test our hypothesis, we examined the ability of wild-type MEK1 or a constitutively activated version to prevent vascular damage *in vivo*. In this study, we demonstrate that overexpression of activated zebrafish MEK1 (MEK1$^{S219D,\ S223D}$ [MEK1DD]) increases phospho-ERK1 and phospho-ERK2 (pERK1/2) levels

* Corresponding author. Mailing address: Vascular Biology Program, Children's Hospital Boston, Karp Family Research Laboratories, 12th Floor, Room 12,217, 1 Blackfan Circle, Boston, MA 02115-5737. Phone: (617) 919-2379. Fax: (617) 730-0231. E-mail: joanne.chan@childrens.harvard.edu.

▽ Published ahead of print on 20 September 2010.

in whole-embryo lysates. We then developed heat shock-inducible transgenic lines for wild-type or activated MEK1. Strikingly, activation of MEK1DD, but not that of wild-type MEK1, prevented LT-induced vascular damage. This genetic approach provides a novel strategy for the examination of the role of host signaling pathways in promoting or impeding pathogen action.

MATERIALS AND METHODS

Animals and reagents. All animal protocols were approved by the Institutional Animal Care and Use Committee of Children's Hospital Boston. Breeding fish were maintained at 28.5°C on a 14-h-light/10-h-dark cycle. Wild-type fish used were of the *AB strain (Oregon), and all transgenic animals were generated in this background. Embryos were collected by natural spawning and were raised in 10% Hanks' saline at 28.5°C unless otherwise indicated.

Antibodies to MEK1/2, pMEK1/2, ERK1/2, pERK1/2, Jun N-terminal protein kinase (JNK), pJNK, p38, and p-p38, as well as anti-mouse or anti-rabbit secondary antibodies, were purchased from Cell Signaling Technology. Sequences used as immunogens were either identical or highly conserved in fish and human homologues. CI-1040 was purchased from Axon Medchem. Recombinant anthrax LF was purchased from List Laboratories, Inc., and PA was generated as described previously (48). Red fluorescent polystyrene microspheres (diameter, 500 nm) were purchased from Thermo Scientific.

Cloning and *in vitro* transcription. Predicted genes for zebrafish MEK1 were provided by the zebrafish genome resources at ensembl.org. High-fidelity PCR (Roche) was used to clone zebrafish MEK1 from cDNA into pTarget expression vectors (Promega). The forward primer sequence was 5′-CCACCATG CAGAAAAGGAGGAAGCCAGAG-3′, and the reverse primer sequence was 5′-GGCTGTTTTCACATTCCCACACTGTGAGTCGGAGTTGCTG-3′. Activated mutants were generated using the QuikChange II site-directed mutagenesis kit (Strategene) and the forward and reverse primer sequences 5′-AGTGGACAACTCATTGACGACATGGCCAATGACTTCGTGGGAA CCAGGTC-3′ and 5′-GACCTGGTTCCCACGAAGTCATTGGCCATGTC GTCAATGAGTTGTCCACT-3′, respectively. Transcripts for wild-type or activated zebrafish MEK1, human MEK1, and the Tol2 transposon were generated using the mMessage mMachine *In Vitro* transcription kit (Ambion). Nucleotide sequences for all constructs described in this paper were determined by the Massachusetts General Hospital's Sequencing Center using the dideoxy method.

***In vitro* translation and LF cleavage assay.** Wild-type MEK1 mRNA transcripts were used to generate zebrafish or human MEK1 proteins with the Reticulocyte Lysate *In Vitro* translation kit (Ambion). Immediately following the completion of *in vitro* translation, 0.5 ng LF was added to 5 μg of the zebrafish or human MEK1 reticulocyte lysate mixture for 30 min at 37°C. The toxin-treated protein preparations were then denatured with sodium dodecyl sulfate (SDS) sample buffer and were incubated at 100°C for 10 min before separation on a 12.5% Tris-HCl gel for 4 h. Size differences in cleaved MEK1 were detected by Western blot analysis using an anti-MEK1/2 antibody.

Transgenesis. Transgenesis constructs were generated using the Tol2 Gateway transgenesis kit (Invitrogen) (30). Briefly, wild-type and constitutively active zebrafish MEK1 cDNA sequences were cloned into the pME-MCS vector. An LR Clonase reaction was then used to recombine the p5E-hsp70i 5′ entry clone, pME-MEK1 or pME-MEK1$^{S219D,\ S223D}$ middle entry clone, and p3E-polyA 3′ entry clone sequences into the pDestTol2CG2 vector, resulting in the generation of the pDestTol2CG2-hsp70i:MEK1 and pDestTol2CG2-hsp70i:MEK1$^{S219D,\ S223D}$ vectors (23, 30).

Zebrafish embryos were injected with 2 nl of 25-ng/μl pDestTol2CG2-hsp70i:MEK1 or pDestTol2CG2-hsp70i:MEK1$^{S219D,\ S223D}$ and 35 ng/μl Tol2 transposon mRNA within 15 min of fertilization. Injected embryos were raised at 25°C until they reached the developmental time point of 48 h postfertilization (hpf) before being selected for both cardiac myosin light chain (CMLC) promoter-driven green fluorescent protein (GFP) expression and wild-type appearance. Selected embryos were then raised for 8 weeks at 28.5°C and were outcrossed with the tg(fli:EGFP) fish line for the generation of F_1 embryos (31). (EGFP is enhanced GFP.) This enabled us to visualize whether beads were extravasated in response to LT action in each line.

PCR, RT-PCR, qPCR, and Western blotting. PCR, reverse transcription-PCR (RT-PCR), and quantitative PCR (qPCR) were carried out using the Qiagen *Taq* DNA polymerase, One-Step RT-PCR, and QuantiFast SYBR green RT-PCR kits, respectively. A primer pair spanning a 3′ portion of zebrafish MEK1 (5′-C GCTGTAGAAAGCCCCATAG-3′) and a region specific to the pME-MCS vector (5′-AAAGGGAACAAAAGCTGGAG-3′) was used for genotypic analysis. RNA was isolated from embryos, 1 h following induction at 47 hpf using Trizol-chloroform extraction, followed by ethanol extraction. Genomic DNA was isolated by incubating embryos in a lysis buffer consisting of 10 mM Tris-HCl (pH 8.0), 50 mM KCl, 0.3% Tween 20, 0.3% Nonidet P-40, and 0.5 mg/ml proteinase K for 12 h at 55°C, followed by 15 min at 98°C. qPCR of genomic DNA was conducted using primers specific to the transgenes (forward, 5′-AGAGGCTGA GGAGGTTGAC-3′; reverse, 5′-AAAGGGAACAAAAGCTGGAG-3′), and comparisons were performed by the $\Delta\Delta CT$ method using β-actin as a reference gene.

Zebrafish embryo protein lysates for Western blot analysis were prepared by first vortexing 20 to 30 embryos per condition for 15 s in calcium-free Ringer's solution and then centrifuging them three times, for 1 min each time, at a relative centrifugal force (RCF) of 13 before the addition of a lysis buffer consisting of 20 mM Tris-HCl (pH 8.0), 1 mM EDTA, 0.5% Nonidet P-40, 300 mM NaCl, 200 μM sodium orthovanadate, and protease inhibitors. Protein concentrations were determined using the Bradford assay, and 75 μg of each lysate was prepared with SDS sample buffer and heated for 10 min at 100°C. Samples were separated on a 7.5% Tris-HCl gel for 1.5 h before being transferred to a nitrocellulose membrane. Membranes were blocked for 1 h with 5% bovine serum albumin (BSA), followed by overnight incubation with the primary antibody in 5% BSA with rocking at 4°C. Blots were then washed and incubated with the secondary antibody for 1 h in 0.5% milk, and the signal was detected using chemiluminescence.

CI-1040 incubation, toxin treatment, and microsphere leakage. Microinjections were carried out as described previously (9). LF and PA were combined immediately before microinjection. Amounts injected for each experiment are indicated in the figure legends. Phenol red (0.05%) was added to the mixture for each condition for visibility during microinjection. Volumes of 40 nl or less were delivered into the common cardinal veins of embryos anesthetized with tricaine (Sigma) at 48 hpf using a gas-driven microinjector (Medical Systems Corp.). After injection, embryos were transferred to fresh medium, and they were scored for LT action at 24 h postinjection (72 hpf).

For the phenocopy of LT effects using a MEK1/2 inhibitor, 2.5 μM CI-1040 was added to the zebrafish embryonic medium at 48 hpf and was then washed out 6 h later. Embryos were scored for phenotypes at 72 hpf as described by Bolcome et al. in 2008 (9).

For the permeability assays, embryos were injected with microspheres at 54 hpf. Extravasation of fluorescent 500-nm-diameter beads from the dorsal aorta was detected by fluorescent microscopy at 72 hpf. Embryos were mounted in 4% methylcellulose before being photographed.

Statistics. Statistical analysis was performed by chi-square tests for zebrafish LT studies in which populations consisting of severe-phenotype, mild-phenotype, and wild-type-appearance embryos were compared (9). The *t* test method was used for all other experiments. Sigma Stat (version 3.0) software was utilized for all statistical analysis. A P value of <0.05 was considered significant.

RESULTS

MEK1 conservation and LF cleavage. We have previously shown that CI-1040, a highly selective and noncompetitive inhibitor for MEK1/2 (50% inhibitory concentration [IC_{50}], 17 nM) (2, 34, 38), could closely phenocopy the effects of LT when administered at the same time point at which the toxin was introduced into the vasculature (Fig. 1) (9). Thus, we hypothesized that overactivation of the MEK1/2-pERK signaling axis might counteract some of the effects of LT entry. To investigate this further, we focused on zebrafish MEK1 and cloned its full-length cDNA (86% identical with human MEK1; GenBank accession number HM031079) (Fig. 2A). Importantly, we demonstrated that the LF cleavage site of MEK1 is conserved and functional. LF activity on zebrafish MEK1 and LF activity on human MEK1 were compared using an *in vitro* translation approach. First, wild-type zebrafish and human MEK1 expression constructs were used to produce mRNA transcripts *in vitro*. The corresponding mRNAs were then used to generate each protein by *in vitro* translation. Finally, the resulting MEK1 proteins were tested for LF cleavage. Each protein preparation was incubated with LF for 30 min before examination by Western blot analysis. We found

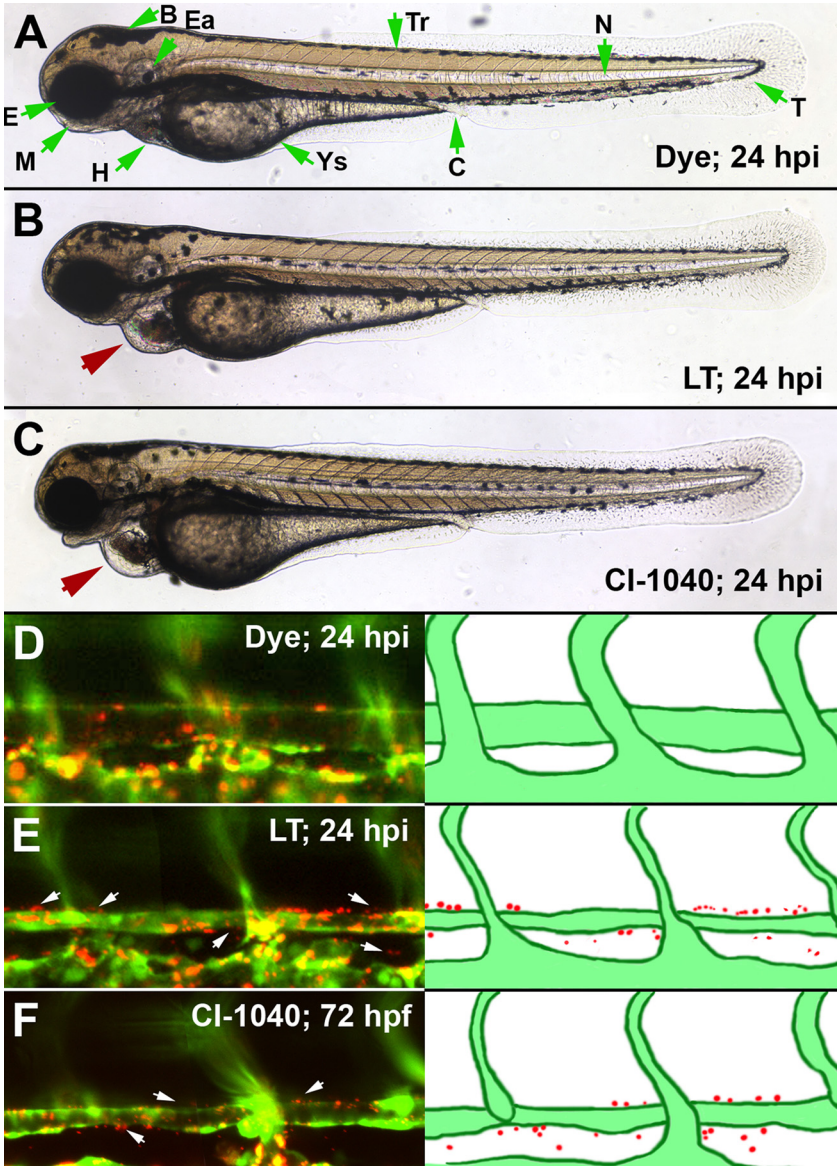

FIG. 1. MEK1/2 inhibition phenocopies LT vascular permeability. An inhibitor for MEK1/2 produces a faithful phenocopy of LT vascular effects. CI-1040 was added to the medium of embryos at the same developmental time point at which we inject LT (48 hpf) and was washed out 6 h later. At 72 hpf, the embryos had pericardial edema, enlarged heart chambers, and vessel collapse (C), all phenotypes that are present in LT-injected embryos (B). In addition, both LT-injected and CI-1040-treated embryos had increased vascular permeability, as detected by the extravasation of 500-nm-diameter microspheres at 72 hpf (E and F). An LT dose of 150 fmol LF and 100 fmol PA was used in these experiments. Red arrows point out the pericardial edema noted in LT- or CI-1040-treated embryos, and white arrows mark regions of extravasated beads. Green arrows indicate morphological features of the zebrafish embryo (A). Abbreviations: B, brain; C, cloaca; Ea, ear; E, eye; H, heart; M, mouth; N, notochord; T, tail; Tr, trunk; Ys, yolk sac.

that both zebrafish MEK1 and human MEK1 were efficiently cleaved by LF, since bands of reduced sizes were observed in the presence of LF (Fig. 2B).

Functional verification of the activated MEK1 construct. The activation of MEK1, as well as its interaction with and subsequent phosphorylation of ERK1/2, has been studied extensively in the cancer field (27, 36). Overexpression of wild-type MEK1 alone is generally not sufficient to increase ERK1/2 phosphorylation and activation, making it necessary to generate constitutively activated mutants for gain-of-function studies (10). Taking advantage of the sequence identity between human and zebrafish MEK1 within the kinase activation loop, we targeted the two Ser residues (Ser219 and Ser223) (Fig. 2A) (10, 16, 51) predicted to be phosphorylated during MEK1 activation (12, 13, 49). We designed a phosphomimetic version of zebrafish MEK1 by substituting Asp for these Ser residues, a strategy that has been used successfully in mammalian studies to generate constitutively active mutants of MEK1 (10). We termed our mutant MEK1DD and tested whether this strategy could be used to activate the MEK1 pathway in zebrafish using mRNA overexpression (Fig. 3).

Owing to the expression of MEK1, ERK1/2, and their roles

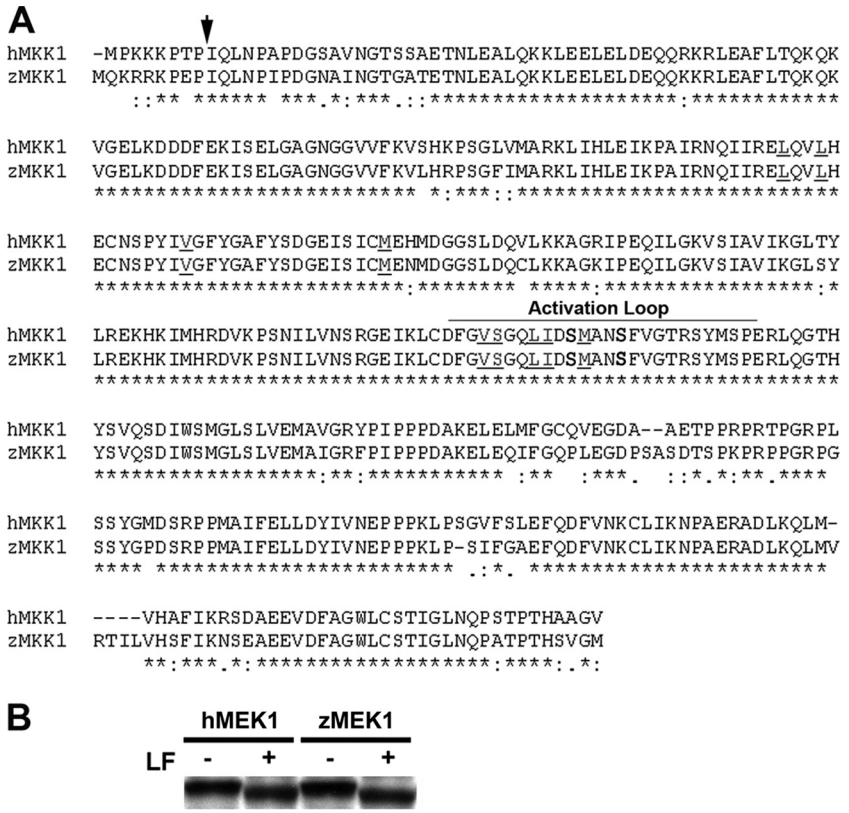

FIG. 2. Zebrafish MEK1/2 orthologues are highly conserved. (A) Alignment of human and zebrafish MEK1 orthologues. An arrow indicates the LF cleavage site; zebrafish residues S219 and S223 are in boldface; residues important to CI-1040–MEK1 binding are underlined; and the activation loop is delineated. Anthrax LF cleaves both zebrafish and human MEK1. (B) Western blot of control and toxin-treated MEK1 protein preparations showing a size shift in those cleaved by LF.

downstream of many receptors, developmental defects are expected from persistent pERK activation (17, 33). We were not surprised to find that MEK1DD overexpression produced severe gastrulation defects; however, its wild-type counterpart caused no obvious phenotype (Fig. 3A to C, F, and H). While the developmental effects caused by MEK1DD could be observed at doses as low as 2 nl of 15-ng/μl mRNA, the wild-type mRNA could be microinjected at >10-fold doses (as high as 200 ng/μl) without inducing detrimental phenotypes (Fig. 3B; also data not shown).

CI-1040 is a noncompetitive inhibitor of MEK1, and sequence conservation with the zebrafish version of the kinase suggested that it could also inhibit activated MEK1DD in zebrafish embryos (38). Interestingly, we were able to attenuate many gastrulation defects of global MEK1 activation by adding CI-1040 to the embryonic medium of MEK1DD mRNA-injected embryos from the 60% epiboly stage to 22 h postfertilization (hpf). Images were taken at 30 hpf to facilitate comparison of embryos at a time point at which the heart and other structures can be clearly visualized (Fig. 3D to I). These data strongly suggested that the MEK1DD construct was activating the MEK1 pathway.

To further verify that this MEK1DD construct indeed produced a constitutively activated version of this kinase, we examined the phosphorylation levels of its target kinases, ERK1/2. Western blot analysis of zebrafish whole-embryo lysates revealed that pERK1/2 levels were higher in MEK1DD-expressing embryos than in those injected with wild-type MEK1 mRNA, confirming that S219D and S223D were indeed activating mutations (Fig. 3J). We also tested whether global MEK1 activation could lead to the increased phosphorylation of related mitogen-activated protein kinases (MAPKs), such as JNK and p38. We found that phospho-JNK and phospho-p38 levels were not significantly altered (Fig. 3J).

Transgenic line founder identification. We proposed that MEK1DD might be able to compensate for the LF cleavage of endogenous MEK1 by continual stimulation of downstream pERK function. Thus, we generated transgenic lines expressing wild-type MEK1 or MEK1DD driven by a heat shock protein 70 (hsp70) promoter (23).

To facilitate analysis, each construct included a fluorescent reporter driven by the CMLC promoter (30), so that cardiac expression of GFP enabled us to visually select embryos with genetic incorporation. F_0 embryos with a normal appearance and fluorescent hearts were selected to be raised as potential founders. After 2 to 3 months, these F_0 founders reached sexual maturity and were outcrossed with the tg(fli:EGFP^{y1}) line to produce embryos for further experimentation and to be raised as an F_1 generation (31). Since endothelial cells are labeled by EGFP in this line, increased vessel permeability can be determined by extravasation of red fluorescent microspheres (9).

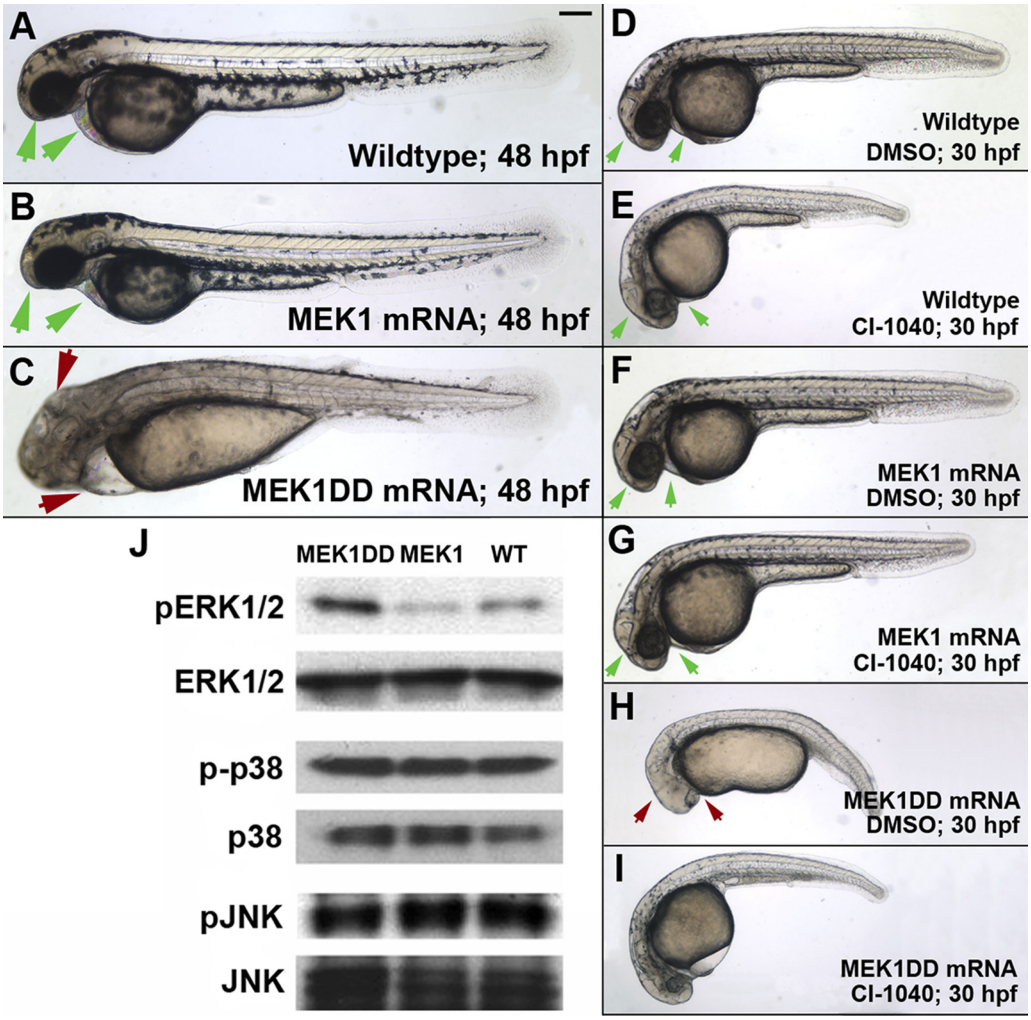

FIG. 3. Global MEK1 activation induces developmental defects. A 2-nl dose of 30-ng/μl wild-type or MEK1DD mRNA was injected into zebrafish embryos immediately following fertilization. (B, C, F, and H) Global expression of wild-type MEK1 induces no obvious developmental defects in zebrafish embryos, while that of activated MEK1 results in gastrulation defects in ~89% of embryos at a dose of 30 ng/μl (C and H) (n, >300 per condition over 4 repeated experiments; P, <0.001). (D to I) CI-1040 could attenuate the gastrulation effects caused by global MEK1DD expression. CI-1040 was added to the embryonic medium from 7 to 24 hpf at a dose of 100 nM. While this dose had minimal effects on wild-type embryos (E), it significantly reduced the developmental effects caused by constitutive MEK1 activation (I) (n, >50 per condition over 3 repeated experiments; P, <0.001). (H) A dimethyl sulfoxide (DMSO) control was unable to attenuate developmental defects. Green arrows, normal head and heart morphology. Red arrows, abnormal head and heart morphology. Bar, 100 μm. (J) MEK1DD expression increases pERK but not pJNK or p-p38 levels in zebrafish embryos, as determined in whole-embryo lysates taken at 24 hpf.

Analysis of inducible MEK1 transgenic lines. The inducible expression of MEK1DD enabled us to bypass the early developmental defects of global MEK1 activation (Fig. 3). Nearly all of the F_1 offspring of hsp70:MEK1DD mosaic founders had a wild-type appearance when raised at 25°C in the absence of heat shock induction. Heat shock induction at early time points resulted in developmental defects similar to those observed upon global induction of the MEK1DD transgene (Fig. 4E and F). No obvious phenotype was noted in the F_1 tg(hsp70:MEK1) embryos of any founder when they were induced in parallel (Fig. 4D). Genomic incorporation and transgene expression were confirmed by PCR and RT-PCR using individual embryos from each line compared to wild-type sibling controls (Fig. 4O). Further, Western blotting for pERK1/2 was used to demonstrate increased ERK1/2 phosphorylation following heat shock induction in tg(hsp70:MEK1DD) embryos compared to that of their wild-type siblings or tg(hsp70:MEK1) embryos (Fig. 4M).

Heat shock induction of MEK1 activation rescues LT effects. The heat shock conditions were optimized to ensure transgene expression both immediately before LT injection and several hours after, with minimal phenotypic effects by 72 hpf. To test whether constitutive activation of MEK1 could alter LT effects, we raised tg(hsp70:MEK1DD) and tg(hsp70:MEK) embryos at 25°C until the 47-hpf developmental stage before heat shock induction at 37°C for 1 h. LT was injected into the vasculature at 48 hpf (Fig. 5). Embryos were induced again from 4 to 5 h postinjection (hpi). Heat shock induction did not cause obvious developmental defects in wild-type or tg(hsp70:MEK1) embryos; however, approximately 25% of

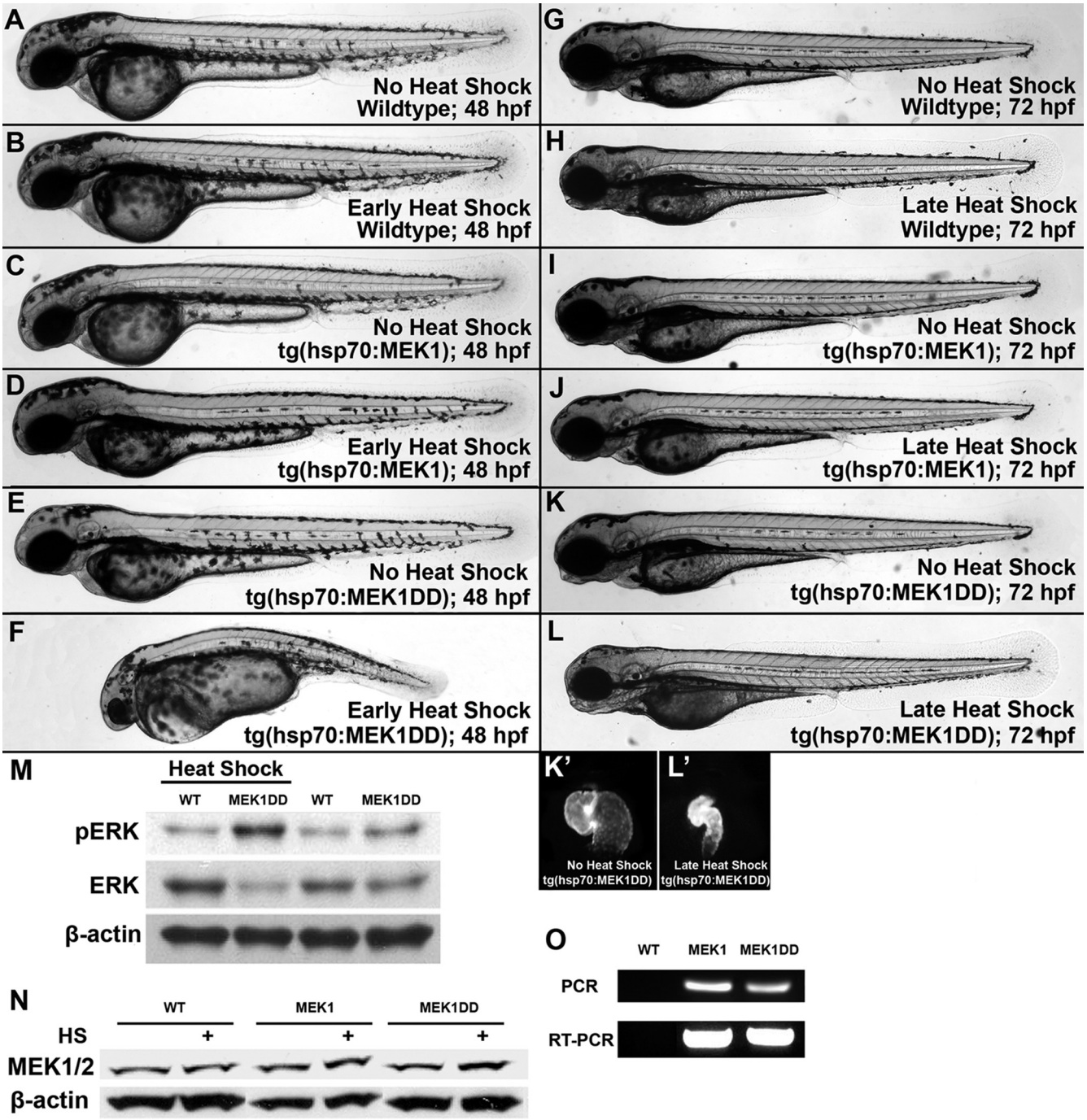

FIG. 4. Phenotypes in inducible transgenic lines are consistent with global activation. Transgenic F_1 embryos expressing activated or wild-type MEK1 under the control of a heat shock protein promoter were generated from our mosaic founders. Wild-type and tg(hsp70:MEK1) embryos had no obvious phenotype after heat shock (A to D), and tg(hsp70:MEK1DD) embryos showed defects 24 h following induction from 6 to 7 hpf (F). Uninduced tg(hsp70:MEK1DD) embryos appeared normal (E). Milder effects were noted in approximately 25% of embryos expressing MEK1DD (*n*, 124), when heat shock induction was performed from 47 to 48 hpf, and again from 52 to 53 hpf (K and L). Obvious effects were limited to the heart, which had a smaller size and impaired function compared to those of uninduced controls (K′ and L′). These heart effects could be visualized due to the CMLC2-driven GFP expression incorporated into our transgenic constructs. Wild-type and tg(hsp70:MEK1) embryos had no obvious defects following late heat shock induction (H and J). (M and O) pERK1/2 levels increased in tg(hsp70:MEK1DD) but not tg(hsp70:MEK1) or sibling embryos 1 h after induction (M), and genomic incorporation and expression of each transgene were verified by PCR and RT-PCR, respectively (O). (N) Heat shock induction for 2 h mildly increased MEK1 protein levels in both heat shock-regulated lines: hsp70:MEK1 and hsp70:MEK1DD.

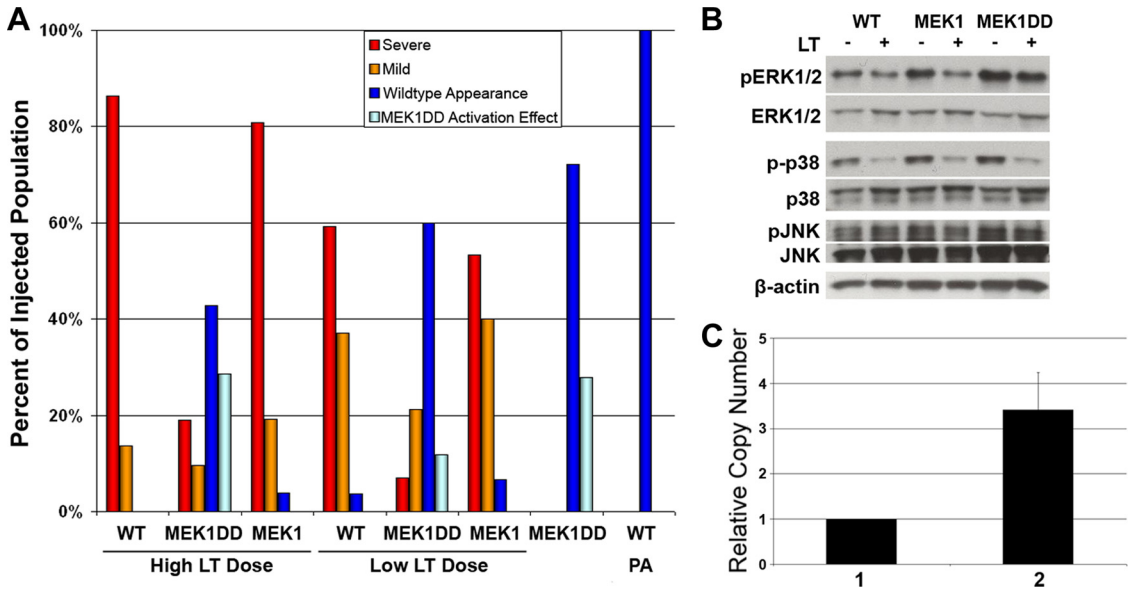

FIG. 5. MEK1 activation rescues LT vascular effects. We selected tg(hsp70:MEK1DD) F_1 embryos for LT assays. (A) Interestingly, induction rescued many of these embryos from LT effects at 24 hpi, while neither induced tg(hsp70:MEK1) nor wild-type sibling embryos were resistant to LT [*n*, >20 per condition, representative of three experiments; *P*, <0.001 for tg(hsp70:MEK1DD) rescue at each LT dose; *P*, 0.659 and 0.089 for tg(hsp70:MEK1) at low and high LT doses, respectively]. For the low LT dose, we used 37 fmol LF and 25 fmol PA; 150 fmol LF and 100 fmol PA were used for the high LT dose. (B) Western blot analysis conducted on whole-embryo lysates collected at 6 hpi showed that pERK1/2 levels, but not pJNK or p-p38 levels, were elevated in tg(hsp70:MEK1DD) embryos following toxin injection. (C) Embryos that were rescued from toxin effects had higher copy numbers of the MEK1DD transgene than those with severe phenotypes. Column 1 represents the copy number of rescued embryos compared with themselves, while column 2 represents the higher copy number of the transgene in rescued embryos than in those with a severe phenotype. Data are from 5 independent experiments using a total of 25 rescued embryos and 20 embryos with a severe phenotype; *P*, 0.012; error bar, standard error.

tg(hsp70:MEK1DD) embryos had compromised circulation due to small hearts that failed to beat normally (Fig. 4L), while the remaining 75% appeared normal. Embryos were scored for toxin phenotypes, as previously described (9). Briefly, embryos with pericardial edema, enlarged heart chambers, collapsed vessels, and no blood circulation were scored as having a "severe" phenotype. Those having each of the toxin phenotypes but retaining some circulation were scored as "mild," and those with a wild-type appearance were recorded as "normal." tg(hsp70:MEK1DD) embryos with smaller hearts after heat shock induction were scored as having a "MEK1DD activation effect." We found that MEK1 activation could rescue embryos from LT effects. While tg(hsp70:MEK1) and uninduced tg(hsp70:MEK1DD) embryos were just as susceptible, or nearly as susceptible, to LT as wild-type embryos, we found that heat shock-induced tg(hsp70:MEK1DD) embryos were resistant to LT effects (Fig. 5A and 6).

Since we were using the F_1 offspring of transgenic founders for our experiments, each embryo could have a different MEK1DD transgene copy number. We hypothesized that embryos with higher transgene copy numbers might be more likely to have a complete rescue of toxin effects than those with lower copy numbers. Primers specific to the activated MEK1 transgene were used to assess the potential correlation between the relative amount of the MEK1 transgene and toxin effects in individual embryos by qPCR. Interestingly, we found that higher transgene copy numbers provided greater protection from toxin effects than lower copy numbers in our embryos (Fig. 5C).

We also investigated whether MEK1 activation was sufficient to attenuate LT-induced vascular leakage by using our microsphere extravasation assay (9). tg(hsp70:MEK1DD), tg(hsp70:MEK1), and wild-type embryos were raised and induced as described above. At 6 hpi, each embryo was injected with microspheres, allowing us to monitor vascular permeability by observing bead extravasation *in vivo*. LT increased microsphere leakage in the dorsal aortae of wild-type and tg(hsp:MEK1) embryos, but not in those of tg(hsp:MEK1DD) embryos (Fig. 6E to H). These data demonstrated an ability of activated MEK1 to prevent LT-induced endothelial leakage, providing strong evidence for the importance of MEK1 to LT action.

While LF has the ability to cleave the MEK1DD protein (data not shown), we found that its activation overcame toxin-induced vascular permeability. Additionally, Western blot analysis confirmed that the level of phosphorylation of ERK1/2, but not that of JNK or p38, was increased in tg(hsp70:MEK1DD) embryos following toxin injection (Fig. 5B). These data suggest that impaired MEK1 signaling to ERK1/2 contributed greatly to LT-induced permeability. Combining this with our data demonstrating that chemical inhibition of MEK1/2 can phenocopy toxin effects, we believe that LT cleavage of MEK1/2 is an important component of vascular leakage in zebrafish embryos. Interestingly, we did not observe a strong decrease in pJNK levels in response to LT. Consequently, we tested whether a specific JNK inhibitor could induce any vascular abnormalities in our model.

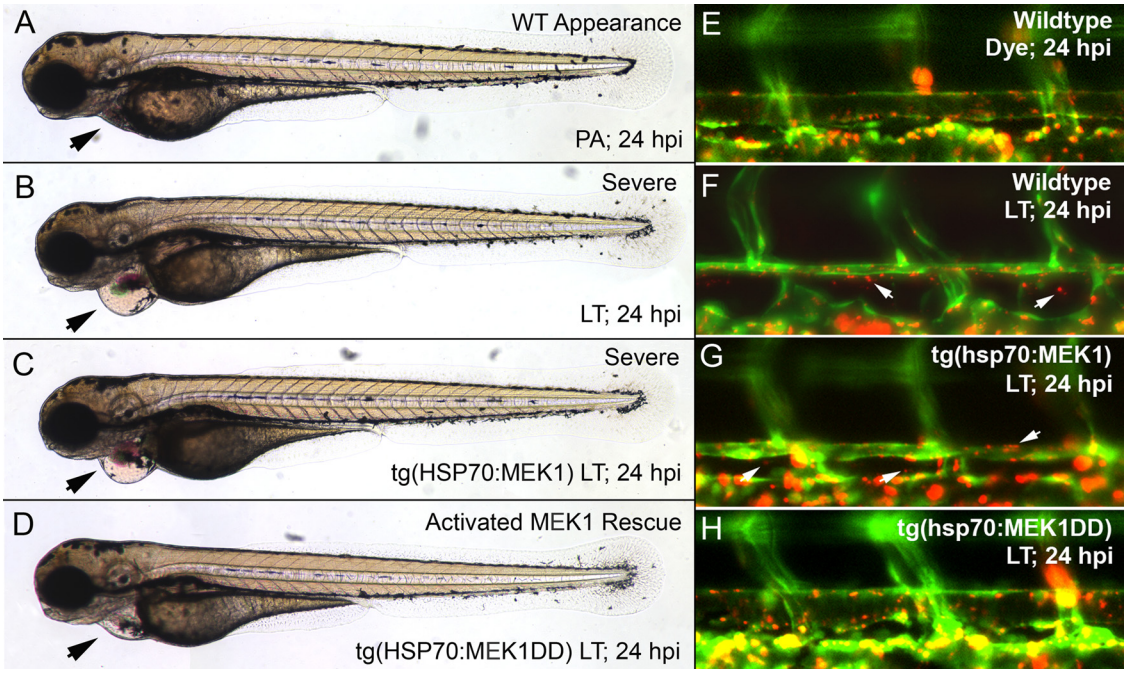

FIG. 6. MEK1 activation attenuates LT effects. While the injection of LT resulted in pericardial edema, enlarged heart chambers, and reduced or absent blood circulation in wild-type and tg(hsp70:MEK1) embryos (B and C), most tg(hsp70:MEK1DD) embryos were rescued from toxin effects (D). Black arrows mark differences in pericardial edema between the lines and treatment conditions used. (E to H) Vascular permeability following LT injection was assessed by testing for the extravasation of fluorescent microspheres in tg(hsp70:MEK1DD), tg(hsp70:MEK1), and wild-type embryos. While bead leakage from the dorsal aorta was detected in wild-type and tg(hsp70:MEK1) embryos (F and G), no bead leakage from tg(hsp70:MEK1DD) transgenic animals was detected (H). An LT dose of 150 fmol LF and 100 fmol PA was used in these experiments.

JNK and p38 inhibitors do not cause vascular effects. Our data demonstrated that LT vascular effects could be phenocopied with an inhibitor specific for MEK1/2 and could be rescued with MEK1 activation; however, attempts at testing the JNK and p38 MAPK pathways did not demonstrate a strong correlation with LT-induced vascular permeability in the fish model. Because chemical inhibitors specific to MEK3/6 and MEK4/7 are not available, we could target only their downstream kinases, JNK and p38. Human and zebrafish JNK and p38 are highly conserved; they are 85 and 88% identical, respectively (comparisons were conducted with the amino acid sequences of JNK1 and p38α). Embryos were treated with SP600125, an inhibitor specific for JNK1/2/3 (IC_{50}, 110 to 190 nM) (7), or SB203580, an inhibitor specific for p38 (IC_{50}, 600 nM) (14), using the same protocol described for CI-1040 (9). Briefly, each drug was added to the embryonic medium from 48 to 54 hpf before being washed out. Embryos were scored at 72 hpf. While a 2.5 μM dose of CI1040 can phenocopy toxin effects in 100% of treated embryos, neither SP600125 or SB203580 produced observable vascular phenotypes at doses as high as 10 μM (Fig. 7C and D). Although SB203580 embryos appeared to be completely wild type, SP600125 did generate some effects on jaw development (Fig. 7C). Western blot analysis revealed that SP600125 completely blocked the phosphorylation of c-JUN, a downstream target of JNK. Unfortunately, antibodies targeting p38 signaling targets were not conserved with zebrafish homologues; thus, we could not verify the efficacy of SB203580. Although inhibition of p38 by SB203580 may be limited by accessibility issues, our data using zebrafish lysates suggest a minor role, because LT vascular effects were prevented by activated MEK1, without p38 levels being restored (Fig. 5B).

DISCUSSION

Toxins produced by *B. anthracis* have been studied for more than 50 years (40); however, little is known about how toxin-induced vascular permeability and edema contribute to multiple-organ dysfunction and death (4, 22, 35, 37, 44). While it has been difficult to investigate LT-induced vascular permeability changes in live mammalian models, we have taken advantage of the zebrafish as a surrogate model to investigate LT-dependent vascular effects *in vivo* (9). The zebrafish provides a valuable alternative vertebrate model, amenable to genetics and chemical biology, to facilitate the study of host signaling pathways for pathogen research. As a vertebrate organism, the zebrafish shares a high degree of functional conservation of genes and signaling pathways with mammals. An additional advantage of the fish model is the ability to use hundreds of embryos, yielding large sample numbers for the examination of several conditions within a single experiment. The embryonic transparency, external fertilization, and rapid development of the zebrafish facilitate the observation of cell biology *in vivo*.

Since anthrax infections affect multiple organs, it seemed logical that immune cells might be involved. Macrophages were shown to be susceptible to LT in the late 1980s and early 1990s, prompting studies on their lysis and/or behavior follow-

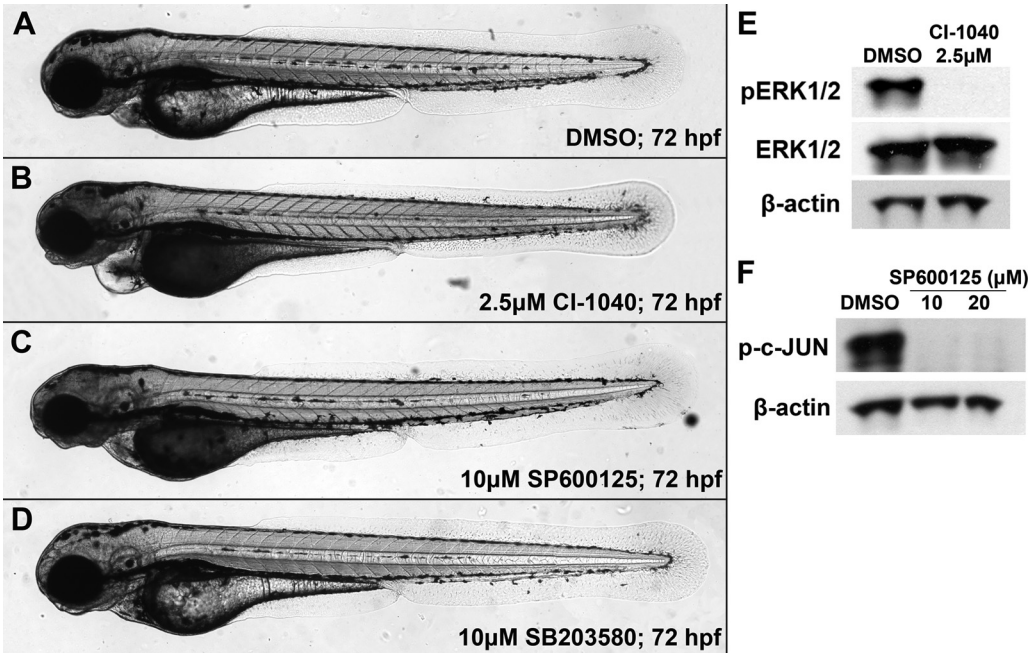

FIG. 7. No vascular phenotype results from JNK or p38 inhibition. (A to D) Embryos were treated with either CI-1040 (an inhibitor of MEK1/2), SB203580 (an inhibitor of p38), or SP600125 (an inhibitor of JNK) from 48 to 54 hpf and were scored at 72 hpf. Only inhibition of MEK1/2 produced a vascular phenotype (B), though JNK inhibition did cause a defect in jaw development (C). p38 inhibition produced no obvious phenotype (D). (E) Western blot analysis revealed that 2.5 μM CI-1040 completely blocked ERK1/2 phosphorylation by the end of the 6-h treatment beginning at 48 hpf, while phosphorylation levels were normal in dimethyl sulfoxide (DMSO) controls. (F) Similarly, SP600125 completely blocked c-JUN phosphorylation after the same treatment regimen. We were unable to provide similar analysis of p38 targets downstream due to the lack of available antibodies.

ing toxin treatment (3, 8, 19, 24–26). However, the precise role of macrophage lysis in systemic LT effects has not been clearly defined (21, 35, 45, 50). In contrast, consistent increases in vascular permeability have been reported in many experimental LT challenge studies in mammals and in human cases of anthrax infections (1, 4, 35).

In recent years, increasing evidence for LT-induced vascular damage has generated interest in defining how blood vessels are affected. It should be noted that rats injected with small amounts of LT die rapidly with severe lung edema, pleural effusions, and cyanosis, suggesting a strong link between vascular involvement and lethality (5, 29, 42, 43). Taking advantage of our zebrafish vascular model, we took initial steps to consider the role of host intracellular signaling pathways affected by LT. The ability of LF to cleave and inactivate one or more MEKs has been clearly demonstrated in cell-based and biochemical assays (18, 39, 47), but investigators have not been able to examine its effects *in vivo*. To determine whether MEK inactivation plays a role in increasing vascular permeability in the zebrafish model, we demonstrated the ability of a highly selective MEK1/2 inhibitor to phenocopy LT effects (9), while available inhibitors of the MEK4/7-driven JNK pathway or the MEK3/6-induced p38 pathway did not generate appreciable effects. Our investigation on the MEK1/2-ERK1/2 signaling pathway continued to generate consistent results using multiple approaches.

Using our model, we also investigated MEK pathway changes independently of chemical inhibitors. We relied on the high level of homology between the MAPKs to examine ERK, JNK, and 38 phosphorylation levels upon LT challenge. In these experiments, both ERK1/2 and p38 signaling appeared strongly affected; however, our MEK1DD experiments demonstrated that increasing pERK1/2 levels was sufficient to rescue LT effects. We note that due to the limitations of available MEK3/6/4/7/JNK/p38 reagents, we cannot definitively determine the contribution of MEK3/6/4/7 inhibition to LT-induced vascular permeability at this point. Since no specific MEK4/7 or MEK3/6 inhibitors are available, we cannot rule out the possibility that other, uncharacterized downstream signaling partners could contribute to vascular effects upon the inactivation of MEK4/7 or MEK3/6. However, our data are consistent with the MEK1/2-ERK1/2 pathway playing an important role in LT vascular effects (9).

In this study, we developed a transgenic zebrafish line, tg(hsp70:MEK1DD), in which a constitutively active MEK1 mutant is driven under the control of a heat shock promoter. To determine whether the LT-induced increase in permeability might be averted in the presence of increased MEK1-ERK signaling, we induced transgene expression at selected time points. Indeed, induction of constitutively active MEK1 either reduced the severity of the vascular effects of LT or prevented them, suggesting that host MEK1-ERK inactivation plays an important role in the deregulation of vascular permeability in our model. We also found that the level of rescue could be directly correlated with the transgene copy number. Western blot analysis confirmed that MEK1DD increased the level of phosphorylation of ERK1/2 without affecting the activation state of JNK or p38, suggesting that the MEK3/6 and MEK4/7

signaling cascades were not grossly affected by the MEK1 gain of function. Finally, expression of MEK1DD was able to rescue both pERK levels and vascular leakage following toxin injection, while the expression of wild-type MEK1 could not. Our work is also in agreement with a cell-based study showing that cleavage of MEK1/2, and not of the related MEKs, was chiefly responsible for increased epithelial cell barrier dysfunction (32). Taken together, these data suggest that LT inactivation of the host MEK1/2–ERK1/2 signaling pathway significantly contributes to vessel collapse and vascular permeability.

Our study demonstrates a novel *in vivo* approach to examining pathogen-host interactions and identifying key host effectors usurped in the process. Since pathogens are generally limited in their genome complexity, it is a common strategy for them to manipulate host proteins for their own benefit. This aspect of pathogen action has been particularly difficult to study in mammalian models. Here we present a visually accessible genetic model that provides an additional strategy to investigate the action of pathogens.

ACKNOWLEDGMENTS

We thank R. J. Collier, T. Roberts, and L. Zon for helpful discussions and/or critical reading of the manuscript. We acknowledge D. Reed for technical assistance.

This work was supported by NIAID and the New England Regional Center of Excellence for Biodefense and Emerging Infectious Diseases (AI057159).

The authors declare no financial conflict of interest that might be construed as influencing the results of this study or their interpretation.

REFERENCES

1. **Abramova, F. A., L. M. Grinberg, O. V. Yampolskaya, and D. H. Walker.** 1993. Pathology of inhalational anthrax in 42 cases from the Sverdlovsk outbreak of 1979. Proc. Natl. Acad. Sci. U. S. A. **90:**2291–2294.
2. **Allen, L. F., J. Sebolt-Leopold, and M. B. Meyer.** 2003. CI-1040 (PD184352), a targeted signal transduction inhibitor of MEK (MAPKK). Semin. Oncol. **30:**105–116.
3. **Banks, D. J., M. Barnajian, F. J. Maldonado-Arocho, A. M. Sanchez, and K. A. Bradley.** 2005. Anthrax toxin receptor 2 mediates Bacillus anthracis killing of macrophages following spore challenge. Cell. Microbiol. **7:**1173–1185.
4. **Beall, F. A., and F. G. Dalldorf.** 1966. The pathogenesis of the lethal effect of anthrax toxin in the rat. J. Infect. Dis. **116:**377–389.
5. **Beall, F. A., M. J. Taylor, and C. B. Thorne.** 1962. Rapid lethal effect in rats of a third component found upon fractionating the toxin of Bacillus anthracis. J. Bacteriol. **83:**1274–1280.
6. **Bélanger, L. F., S. Roy, M. Tremblay, B. Brott, A. M. Steff, W. Mourad, P. Hugo, R. Erikson, and J. Charron.** 2003. Mek2 is dispensable for mouse growth and development. Mol. Cell. Biol. **23:**4778–4787.
7. **Bennett, B. L., D. T. Sasaki, B. W. Murray, E. C. O'Leary, S. T. Sakata, W. Xu, J. C. Leisten, A. Motiwala, S. Pierce, Y. Satoh, S. S. Bhagwat, A. M. Manning, and D. W. Anderson.** 2001. SP600125, an anthrapyrazolone inhibitor of Jun N-terminal kinase. Proc. Natl. Acad. Sci. U. S. A. **98:**13681–13686.
8. **Bhatnagar, R., Y. Singh, S. H. Leppla, and A. M. Friedlander.** 1989. Calcium is required for the expression of anthrax lethal toxin activity in the macrophagelike cell line J774A.1. Infect. Immun. **57:**2107–2114.
9. **Bolcome, R. E., III, S. E. Sullivan, R. Zeller, A. P. Barker, R. J. Collier, and J. Chan.** 2008. Anthrax lethal toxin induces cell death-independent permeability in zebrafish vasculature. Proc. Natl. Acad. Sci. U. S. A. **105:**2439–2444.
10. **Brunet, A., G. Pages, and J. Pouyssegur.** 1994. Constitutively active mutants of MAP kinase kinase (MEK1) induce growth factor-relaxation and oncogenicity when expressed in fibroblasts. Oncogene **9:**3379–3387.
11. **Collier, R. J., and J. A. Young.** 2003. Anthrax toxin. Annu. Rev. Cell Dev. Biol. **19:**45–70.
12. **Crews, C. M., A. Alessandrini, and R. L. Erikson.** 1992. The primary structure of MEK, a protein kinase that phosphorylates the ERK gene product. Science **258:**478–480.
13. **Crews, C. M., and R. L. Erikson.** 1992. Purification of a murine protein-tyrosine/threonine kinase that phosphorylates and activates the Erk-1 gene product: relationship to the fission yeast byr1 gene product. Proc. Natl. Acad. Sci. U. S. A. **89:**8205–8209.
14. **Cuenda, A., J. Rouse, Y. N. Doza, R. Meier, P. Cohen, T. F. Gallagher, P. R. Young, and J. C. Lee.** 1995. SB 203580 is a specific inhibitor of a MAP kinase homologue which is stimulated by cellular stresses and interleukin-1. FEBS Lett. **364:**229–233.
15. **Cui, X., M. Moayeri, Y. Li, X. Li, M. Haley, Y. Fitz, R. Correa-Araujo, S. M. Banks, S. H. Leppla, and P. Q. Eichacker.** 2004. Lethality during continuous anthrax lethal toxin infusion is associated with circulatory shock but not inflammatory cytokine or nitric oxide release in rats. Am. J. Physiol. Regul. Integr. Comp. Physiol. **286:**R699–R709.
16. **Deak, J. C., and D. J. Templeton.** 1997. Regulation of the activity of MEK kinase 1 (MEKK1) by autophosphorylation within the kinase activation domain. Biochem. J. **322**(Pt. 1)**:**185–192.
17. **Dentici, M. L., A. Sarkozy, F. Pantaleoni, C. Carta, F. Lepri, R. Ferese, V. Cordeddu, S. Martinelli, S. Briuglia, M. C. Digilio, G. Zampino, M. Tartaglia, and B. Dallapiccola.** 2009. Spectrum of MEK1 and MEK2 gene mutations in cardio-facio-cutaneous syndrome and genotype-phenotype correlations. Eur. J. Hum. Genet. **17:**733–740.
18. **Duesbery, N. S., C. P. Webb, S. H. Leppla, V. M. Gordon, K. R. Klimpel, T. D. Copeland, N. G. Ahn, M. K. Oskarsson, K. Fukasawa, K. D. Paull, and G. F. Vande Woude.** 1998. Proteolytic inactivation of MAP-kinase-kinase by anthrax lethal factor. Science **280:**734–737.
19. **Friedlander, A. M., R. Bhatnagar, S. H. Leppla, L. Johnson, and Y. Singh.** 1993. Characterization of macrophage sensitivity and resistance to anthrax lethal toxin. Infect. Immun. **61:**245–252.
20. **Giroux, S., M. Tremblay, D. Bernard, J. F. Cardin-Girard, S. Aubry, L. Larouche, S. Rousseau, J. Huot, J. Landry, L. Jeannotte, and J. Charron.** 1999. Embryonic death of Mek1-deficient mice reveals a role for this kinase in angiogenesis in the labyrinthine region of the placenta. Curr. Biol. **9:**369–372.
21. **Golden, H. B., L. E. Watson, H. Lal, S. K. Verma, D. M. Foster, S. R. Kuo, A. Sharma, A. Frankel, and D. E. Dostal.** 2009. Anthrax toxin: pathologic effects on the cardiovascular system. Front. Biosci. **14:**2335–2357.
22. **Guarner, J., J. A. Jernigan, W. J. Shieh, K. Tatti, L. M. Flannagan, D. S. Stephens, T. Popovic, D. A. Ashford, B. A. Perkins, and S. R. Zaki.** 2003. Pathology and pathogenesis of bioterrorism-related inhalational anthrax. Am. J. Pathol. **163:**701–709.
23. **Halloran, M. C., M. Sato-Maeda, J. T. Warren, F. Su, Z. Lele, P. H. Krone, J. Y. Kuwada, and W. Shoji.** 2000. Laser-induced gene expression in specific cells of transgenic zebrafish. Development **127:**1953–1960.
24. **Hanna, P. C., D. Acosta, and R. J. Collier.** 1993. On the role of macrophages in anthrax. Proc. Natl. Acad. Sci. U. S. A. **90:**10198–10201.
25. **Hanna, P. C., S. Kochi, and R. J. Collier.** 1992. Biochemical and physiological changes induced by anthrax lethal toxin in J774 macrophage-like cells. Mol. Biol. Cell **3:**1269–1277.
26. **Hanna, P. C., B. A. Kruskal, R. A. Ezekowitz, B. R. Bloom, and R. J. Collier.** 1994. Role of macrophage oxidative burst in the action of anthrax lethal toxin. Mol. Med. **1:**7–18.
27. **Johnson, G. L., H. G. Dohlman, and L. M. Graves.** 2005. MAPK kinase kinases (MKKKs) as a target class for small-molecule inhibition to modulate signaling networks and gene expression. Curr. Opin. Chem. Biol. **9:**325–331.
28. **Juris, S. J., R. A. Melnyk, R. E. Bolcome III, J. Chan, and R. J. Collier.** 2007. Cross-linked forms of the isolated N-terminal domain of the lethal factor are potent inhibitors of anthrax toxin. Infect. Immun. **75:**5052–5058.
29. **Kuo, S. R., M. C. Willingham, S. H. Bour, E. A. Andreas, S. K. Park, C. Jackson, N. S. Duesbery, S. H. Leppla, W. J. Tang, and A. E. Frankel.** 2008. Anthrax toxin-induced shock in rats is associated with pulmonary edema and hemorrhage. Microb. Pathog. **44:**467–472.
30. **Kwan, K. M., E. Fujimoto, C. Grabher, B. D. Mangum, M. E. Hardy, D. S. Campbell, J. M. Parant, H. J. Yost, J. P. Kanki, and C. B. Chien.** 2007. The Tol2kit: a multisite gateway-based construction kit for Tol2 transposon transgenesis constructs. Dev. Dyn. **236:**3088–3099.
31. **Lawson, N. D., and B. M. Weinstein.** 2002. In vivo imaging of embryonic vascular development using transgenic zebrafish. Dev. Biol. **248:**307–318.
32. **Lehmann, M., D. Noack, M. Wood, M. Perego, and U. G. Knaus.** 2009. Lung epithelial injury by B. anthracis lethal toxin is caused by MKK-dependent loss of cytoskeletal integrity. PLoS One **4:**e4755.
33. **Lorenz, K., J. P. Schmitt, M. Vidal, and M. J. Lohse.** 2009. Cardiac hypertrophy: targeting Raf/MEK/ERK1/2-signaling. Int. J. Biochem. Cell Biol. **41:**2351–2355.
34. **Lorusso, P. M., A. A. Adjei, M. Varterasian, S. Gadgeel, J. Reid, D. Y. Mitchell, L. Hanson, P. DeLuca, L. Bruzek, J. Piens, P. Asbury, K. Van Becelaere, R. Herrera, J. Sebolt-Leopold, and M. B. Meyer.** 2005. Phase I and pharmacodynamic study of the oral MEK inhibitor CI-1040 in patients with advanced malignancies. J. Clin. Oncol. **23:**5281–5293.
35. **Moayeri, M., D. Haines, H. A. Young, and S. H. Leppla.** 2003. Bacillus anthracis lethal toxin induces TNF-α-independent hypoxia-mediated toxicity in mice. J. Clin. Invest. **112:**670–682.
36. **Morrison, D. K., and R. J. Davis.** 2003. Regulation of MAP kinase signaling modules by scaffold proteins in mammals. Annu. Rev. Cell Dev. Biol. **19:**91–118.
37. **Nordberg, B. K., C. G. Schmiterloew, B. Bergrahm, and H. Lundstroem.** 1964. Further pathophysiological investigations into the terminal course of

experimental anthrax in the rabbit. Acta Pathol. Microbiol. Scand. **60:**108–116.

38. **Ohren, J. F., H. Chen, A. Pavlovsky, C. Whitehead, E. Zhang, P. Kuffa, C. Yan, P. McConnell, C. Spessard, C. Banotai, W. T. Mueller, A. Delaney, C. Omer, J. Sebolt-Leopold, D. T. Dudley, I. K. Leung, C. Flamme, J. Warmus, M. Kaufman, S. Barrett, H. Tecle, and C. A. Hasemann.** 2004. Structures of human MAP kinase kinase 1 (MEK1) and MEK2 describe novel noncompetitive kinase inhibition. Nat. Struct. Mol. Biol. **11:**1192–1197.
39. **Pellizzari, R., C. Guidi-Rontani, G. Vitale, M. Mock, and C. Montecucco.** 1999. Anthrax lethal factor cleaves MKK3 in macrophages and inhibits the LPS/IFNγ-induced release of NO and TNFα. FEBS Lett. **462:**199–204.
40. **Ross, J. M.** 1955. On the histopathology of experimental anthrax in the guinea-pig. Br. J. Exp. Pathol. **36:**336–339.
41. **Scholl, F. A., P. A. Dumesic, D. I. Barragan, K. Harada, V. Bissonauth, J. Charron, and P. A. Khavari.** 2007. Mek1/2 MAPK kinases are essential for mammalian development, homeostasis, and Raf-induced hyperplasia. Dev. Cell **12:**615–629.
42. **Scobie, H. M., D. Thomas, J. M. Marlett, G. Destito, D. J. Wigelsworth, R. J. Collier, J. A. Young, and M. Manchester.** 2005. A soluble receptor decoy protects rats against anthrax lethal toxin challenge. J. Infect. Dis. **192:**1047–1051.
43. **Scobie, H. M., D. J. Wigelsworth, J. M. Marlett, D. Thomas, G. J. Rainey, D. B. Lacy, M. Manchester, R. J. Collier, and J. A. Young.** 2006. Anthrax toxin receptor 2-dependent lethal toxin killing in vivo. PLoS Pathog. **2:**e111.
44. **Stearns-Kurosawa, D. J., F. Lupu, F. B. Taylor, Jr., G. Kinasewitz, and S. Kurosawa.** 2006. Sepsis and pathophysiology of anthrax in a nonhuman primate model. Am. J. Pathol. **169:**433–444.
45. **Terra, J. K., C. K. Cote, B. France, A. L. Jenkins, J. A. Bozue, S. L. Welkos, S. M. LeVine, and K. A. Bradley.** 2010. Resistance to Bacillus anthracis infection mediated by a lethal toxin sensitive allele of Nalp1b/Nlrp1b. J. Immunol. **184:**17–20.
46. **Tonello, F., L. Naletto, V. Romanello, F. Dal Molin, and C. Montecucco.** 2004. Tyrosine-728 and glutamic acid-735 are essential for the metalloproteolytic activity of the lethal factor of Bacillus anthracis. Biochem. Biophys. Res. Commun. **313:**496–502.
47. **Vitale, G., L. Bernardi, G. Napolitani, M. Mock, and C. Montecucco.** 2000. Susceptibility of mitogen-activated protein kinase kinase family members to proteolysis by anthrax lethal factor. Biochem. J. **352**(Pt. 3)**:**739–745.
48. **Wigelsworth, D. J., B. A. Krantz, K. A. Christensen, D. B. Lacy, S. J. Juris, and R. J. Collier.** 2004. Binding stoichiometry and kinetics of the interaction of a human anthrax toxin receptor, CMG2, with protective antigen. J. Biol. Chem. **279:**23349–23356.
49. **Wu, J., J. K. Harrison, L. A. Vincent, C. Haystead, T. A. Haystead, H. Michel, D. F. Hunt, K. R. Lynch, and T. W. Sturgill.** 1993. Molecular structure of a protein-tyrosine/threonine kinase activating p42 mitogen-activated protein (MAP) kinase: MAP kinase kinase. Proc. Natl. Acad. Sci. U. S. A. **90:**173–177.
50. **Wu, W., H. Mehta, K. Chakrabarty, J. L. Booth, E. S. Duggan, K. B. Patel, J. D. Ballard, K. M. Coggeshall, and J. P. Metcalf.** 2009. Resistance of human alveolar macrophages to Bacillus anthracis lethal toxin. J. Immunol. **183:**5799–5806.
51. **Xu, S., D. Robbins, J. Frost, A. Dang, C. Lange-Carter, and M. H. Cobb.** 1995. MEKK1 phosphorylates MEK1 and MEK2 but does not cause activation of mitogen-activated protein kinase. Proc. Natl. Acad. Sci. U. S. A. **92:**6808–6812.
52. **Young, J. A., and R. J. Collier.** 2007. Anthrax toxin: receptor binding, internalization, pore formation, and translocation. Annu. Rev. Biochem. **76:**243–265.

Editor: J. B. Bliska